International Journal of Innovative Computing, Information and Control
Volume **8**, Number **3**, March **2012**
ICIC International ©2011 ISSN 1349-4198
pp. –

TOWARD STOCHASTIC EXPLANATION OF A NEUTRALLY STABLE DELAYED FEEDBACK MODEL OF HUMAN BALANCE CONTROL

Katsutoshi Yoshida[1] and Atsushi Higeta[2]

[1]Department of Mechanical and Intelligent Engineering
[2]Department of Innovation Systems Engineering
Utsunomiya University
7-1-2 Yoto, Utsunomiya-shi, Tochigi 321-8585, Japan
yoshidak@cc.utsunomiya-u.ac.jp; higeta@katzlab.jp

Received March 2011; revised September 2011

Abstract. *A stochastic explanation is provided to investigate how human subjects maximize robustness of their balance control while exhibiting on–off intermittent behavior. To this end, the human balance control is modeled by an inverted pendulum with random delayed state feedback. Stochastic analysis based on Lyapunov exponents demonstrates that the on–off intermittency can arise under a neutrally stable condition. Furthermore, the frequency response of statistical moments is derived to show that the neutrally stable condition can be caused by a trade-off between maximal robustness and minimal phase-shift from the disturbance to the second moments.*
Keywords: Human balance control, On–off intermittency, Robust analysis, Lyapunov exponent, Statistical moment, Frequency response

1. **Introduction.** One of the most marvelous features of human balance control is the presence of on–off intermittency in balancing errors [1, 2]. In general, on–off intermittent behavior can arise in the system in a neutrally stable state [3]. This means that the human balance control system might be specifically tuned to be minimally stable. Such a stability design is rarely obtainable from common approaches in control engineering because sufficient stability margins must be designed to achieve stable transient responses. The question arises as to what kind of performance humans prefer to optimize rather than seeking asymptotic stability. We expect that finding the answer will provide new insight for understanding the human-like dynamics of welfare equipment, home care robots, and related devices.

The presence of randomness in human balance control has been explored in the studies on human sway control during quiet standing. It has been revealed that the human body during quiet standing continually moves about in a random fashion [4], and that the fluctuation-dissipation theorem can be applied to the human postural control system [5]. Furthermore, it has also been reported that input noise can be used to improve human balance control [6], based on the mechanism of stochastic resonance [7], which is one of the most typical examples of noise-induced order [8].

Recently, researchers have recognized an additional feature of human balance control, on–off intermittency. It has already been shown that the on–off intermittency arising in human balance control can be modeled precisely by an inverted pendulum with a randomly fluctuated time-delayed feedback controller [1], and that the statistical properties of human stick balancing can be characterized as a special type of random walk, referred to as a Lévy flight. Further, it has been statistically proved that the Lévy flight is deeply connected with the learning process for humans to learn to improve their balance control [2].

As mentioned in the opening paragraph, since the on–off intermittent behavior arises in the system nearly neutrally stable [3], the on–off intermittency generated by humans implies, as reported in the literature [1, 2], that human balance control is tuned near the minimally stable condition.

In the present paper, we investigate the open problem of how human balance control prefers minimal stability. To this end, we focus on the frequency responses of a model of human balance control [1]. A similar viewpoint can be found in the literature [9] based on direct numerical simulations. In contrast, the primary approach used in the present study is based on the theory of stochastic processes. The effectiveness of our stochastic approach has already been demonstrated in previous studies, such as the stability analysis of noise-induced synchronization [10, 11] and coupled human balancing [12]. In contrast to measurement and numerical approaches [1, 9], our analytical approach will provide an explicit mathematical criteria for human-like dynamics that is applicable to modeling human dynamics [13], designing human-like interactive robots [14, 15], and so forth.

In practice, we derive a system of stochastic differential equations (SDE) representing the randomly time-delayed inverted pendulum model [1]. This SDE enables us to calculate Lyapunov exponents [16] evaluating the minimal stability of sample paths of balancing errors analytically. We also derive the moment equations [17] from the SDE to obtain the frequency response of statistical moments of the balancing errors. Based on these results, we will provide a stochastic explanation that the minimally stable condition seems to be caused by a trade-off between maximal robustness and minimal phase-shift from the disturbance to the second moments.

2. **Analytical Model.**

2.1. **Inverted pendulum.**

The equation of motion of an inverted pendulum whose pivot point is mounted on a cart is given by

$$\begin{cases} (M_1+M_2)\ddot{x}+(M_2 l\cos\theta)\ddot{\theta}-M_2 l\dot{\theta}^2\sin\theta+c_x\dot{x}=F(t), \\ (M_2 l\cos\theta)\ddot{x}+(M_2 l^2)\ddot{\theta}-M_2 lg\sin\theta+c\dot{\theta}=0, \end{cases} \tag{1}$$

where M_1 and M_2 are respectively the masses of the cart and the pendulum, l is the length of the rod (considered massless), θ is the slant angle of the pendulum, x is the horizontal displacement of the cart, and c and c_x are respectively the damping coefficients with respect to θ and x. For simplicity, assuming,

$$|\theta|, |\dot{\theta}| \ll 1, \quad M_1 = M_2 = M, \quad c_x = 0, \tag{2}$$

we obtain a linearized equation of motion with respect to the slant angle θ,

$$\ddot{\theta}+\frac{2c}{Ml^2}\dot{\theta}-\frac{2g}{l}\theta=-\frac{1}{Ml}F(t) \tag{3}$$

in which the cart displacement x has vanished due to the linear approximation.

Using the natural frequency $\omega_n=\sqrt{2g/l}$, we perform a temporal scale transformation:

$$t \longmapsto \omega_n^{-1} t. \tag{4}$$

Then, the equation of motion is reduced to the following form:

$$\ddot{\theta}+2\zeta\dot{\theta}-\theta=f(t), \tag{5}$$

where $\zeta = c/(Ml^2\omega_n)$ is the damping ratio and $f(t) = -F(t/\omega_n)/(Ml\omega_n^2)$ is an external torque applied to the pendulum. The non-dimensional torque $f(t)$ is regarded as the combination

$$f(t) = u(t) + v(t), \tag{6}$$

where $u(t)$ is a control input and $v(t)$ is an external disturbance.

2.2. **Random delayed feedback.** It has been reported that the on–off intermittent behavior of human balance control can be precisely modeled by a randomly fluctuated time-delayed feedback controller [1],

$$u(t) = -R_t\,\theta(t-\tau), \quad R_t = K + \sigma\, w_t, \tag{7}$$

where R_t is a random gain with mean K and variance σ^2, and w_t is a standard Gaussian white noise. In order to convert the delayed differential equation into an ordinary differential equation (ODE), we assume $\tau \ll 1$ and expand the delayed term in (7) as

$$u(t) \approx -R_t\left(\theta(t) - \dot\theta(t)\tau\right) = -K\,\theta + (K\tau)\dot\theta - w_t\Big(\sigma\theta - (\sigma\tau)\dot\theta\Big). \tag{8}$$

Note that such linear approximation of delayed variables is often used in engineering applications such as machining chatter analysis [18].

Substituting (8) into (5) through (6), we obtain a state space expression of our model in the following form:

$$\begin{aligned}
&\dot{\boldsymbol{x}} = A\boldsymbol{x} + \boldsymbol{b}\,v(t) + \sigma(D\boldsymbol{x})w_t, \quad \boldsymbol{x} = (\theta, \dot\theta)^T,\\
&A = \begin{bmatrix} 0 & 1 \\ 1-K & K\tau - 2\zeta \end{bmatrix}, \ \boldsymbol{b} = \begin{bmatrix} 0 \\ 1 \end{bmatrix}, \ D = \begin{bmatrix} 0 & 0 \\ -1 & \tau \end{bmatrix}.
\end{aligned} \tag{9}$$

3. **Stability of Sample Paths.**

3.1. **Standard form.** In the following, we denote the eigenvalues of matrix A in (9) as

$$\lambda_\pm = \gamma \pm \sqrt{H}, \tag{10}$$

where

$$\gamma = \frac{1}{2}(K\tau - 2\zeta), \quad H = \frac{1}{4}\left((K\tau - 2\zeta)^2 + 4(1-K)\right).$$

In the case of A having a pair of complex eigenvalues, the system matrices of the linear system (9) can be reduced to the following form:

$$\begin{aligned}
&T_C = \begin{bmatrix} 1 & 0 \\ \gamma & -\sqrt{-H} \end{bmatrix}, \quad A_C = T_C^{-1} A T_C = \begin{bmatrix} \gamma & -\sqrt{-H} \\ \sqrt{-H} & \gamma \end{bmatrix},\\
&\boldsymbol{b}_C = T_C^{-1}\boldsymbol{b} = \frac{1}{\sqrt{-H}}\begin{bmatrix} 0 \\ -1 \end{bmatrix}, \quad D_C = T_C^{-1} D T = \begin{bmatrix} 0 & 0 \\ (1-\gamma\tau)/\sqrt{-H} & \tau \end{bmatrix}.
\end{aligned} \tag{11}$$

In the case of A having two distinct real eigenvalues, the matrices are given by

$$\begin{aligned}
&T_R = \begin{bmatrix} 1 & 1 \\ \lambda_+ & \lambda_- \end{bmatrix}, \quad A_R = T_R^{-1} A T_R = \begin{bmatrix} \lambda_+ & 0 \\ 0 & \lambda_- \end{bmatrix},\\
&\boldsymbol{b}_R = T_R^{-1}\boldsymbol{b} = \frac{1}{2\sqrt{H}}\begin{bmatrix} 1 \\ -1 \end{bmatrix}, \quad D_R = T_R^{-1} D T_R = \frac{1}{2\sqrt{H}}\begin{bmatrix} \lambda_+\tau - 1 & \lambda_-\tau - 1 \\ 1 - \lambda_+\tau & 1 - \lambda_-\tau \end{bmatrix}.
\end{aligned} \tag{12}$$

3.2. Lyapunov exponents. The random ODE in (9) can be rewritten as an SDE of the state $\boldsymbol{x} = (\theta, \dot{\theta})^T$ in the Stratonovich form

$$d\boldsymbol{x} = (A\boldsymbol{x} + \boldsymbol{b}\, v(t))\, dt + (\sigma D\boldsymbol{x}) \circ dW_t, \tag{13}$$

where W_t is a standard Brownian motion. By assuming $v(t) = 0$ and $\sigma \ll 1$, the Lyapunov exponent can be calculated in the following manner [16].

In the case of A having a pair of complex eigenvalues, $D = D_C$, the Lyapunov exponent is given by

$$\lambda^\sigma = \gamma + \frac{\sigma^2}{8} g_1 + o(\sigma^2), \quad g_1 = (D_{12} + D_{21})^2 + (D_{22} - D_{11})^2. \tag{14}$$

In the case of A having two distinct real eigenvalues, $D = D_R$, the Lyapunov exponent is given by

$$\lambda^\sigma = \lambda_+ + \frac{\sigma^2}{2} g_1 + o(\sigma^2), \quad g_1 = D_{12} D_{21}, \tag{15}$$

where D_{ij} is the (i, j)-th element of the matrix D.

4. Frequency Response of Moments. In order to utilize the Itô formula, the Stratonovich-type equation (13) is converted into that of Itô type, which has the following form:

$$d\boldsymbol{x} = \Big((A + \Delta A)\, \boldsymbol{x} + \boldsymbol{b}\, v(t) \Big) dt + (\sigma D\boldsymbol{x}) dW_t, \tag{16}$$

where $\Delta A = (\sigma D)^2/2$ is a drift correction term. Then, the statistical moments of (16) can be derived as follows [17], in which the ensemble average $\langle h(\boldsymbol{x}) \rangle$ of a scalar function $h(\boldsymbol{x})$ such that $h(\mathbf{0}) = 0$ satisfies

$$\frac{d\langle h(\boldsymbol{x})\rangle}{dt} = \big\langle L\big(h(\boldsymbol{x})\big)\big\rangle, \tag{17}$$

where

$$L(\,\cdot\,) = \Big\{ (A + \Delta A)\boldsymbol{x} + \boldsymbol{b} v(t) \Big\}^T \frac{\partial(\,\cdot\,)}{\partial \boldsymbol{x}} + \frac{\sigma^2}{2} \operatorname{tr} \Big\{ (D\boldsymbol{x})^T \frac{\partial}{\partial \boldsymbol{x}} \Big(\frac{\partial(\,\cdot\,)}{\partial \boldsymbol{x}} \Big)^T (D\boldsymbol{x}) \Big\} \tag{18}$$

is used as a generating operator.

4.1. Moment differential equations. Substituting $h(\boldsymbol{x}) = x_1, x_2, x_1^2, x_1 x_2, x_2^2$ into (17), we obtain moment differential equations (MDE) in the following form:

$$\begin{cases} \dot{m}_1 = m_2, \\ \dot{m}_2 = -k\, m_1 - c\, m_2 + v(t), \\ \dot{m}_{11} = 2m_{12}, \\ \dot{m}_{12} = -k\, m_{11} - c\, m_{12} + m_1 v(t), \\ \dot{m}_{22} = \sigma^2 m_{11} + p\, m_{12} + q\, m_{22} + 2v(t)\, m_2, \end{cases} \tag{19}$$

where

$$k = K - 1 + \frac{1}{2}\sigma^2\tau, \quad c = 2\zeta - K\tau - \frac{1}{2}\sigma^2\tau^2, \quad p = 2k - 2\sigma^2\tau, \quad q = -2c + \sigma^2\tau^2 \tag{20}$$

and $m_i = \langle x_i \rangle$ and $m_{ij} = \langle x_i x_j \rangle$ $(i, j = 1, 2)$ are ensemble averages of the state variables. Rewriting the second moments in (19) as variances around mean values, i.e., $s_{ij} = \langle (x_i -$

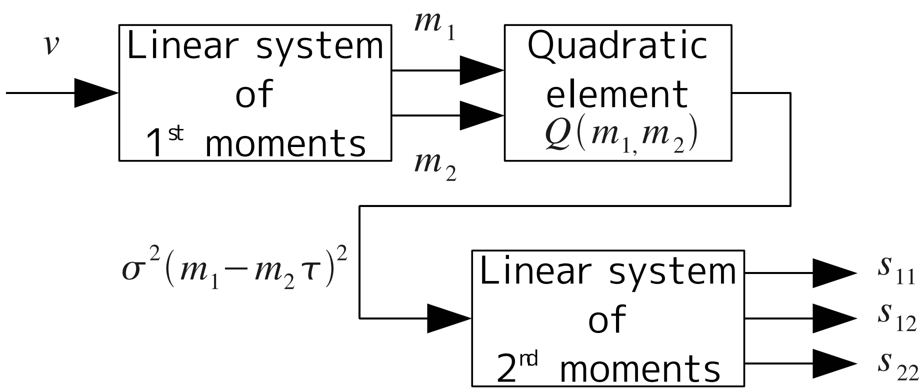

FIGURE 1. Block diagram of MDE

$m_i)(x_j - m_j)\rangle$ $(i, j = 1, 2)$, we obtain

$$\begin{cases} \dot{m}_1 = m_2, \\ \dot{m}_2 = -k\, m_1 - c\, m_2 + v(t), \\ \dot{s}_{11} = 2s_{12}, \\ \dot{s}_{12} = -k\, s_{11} - c\, s_{12} + s_{22}, \\ \dot{s}_{22} = \sigma^2 s_{11} + p\, s_{12} + q\, s_{22} + \sigma^2 (m_1 - m_2\tau)^2. \end{cases} \tag{21}$$

Finally, taking the subspaces $\boldsymbol{m} = (m_1, m_2)^T$ and $\boldsymbol{s} = (s_{11}, s_{12}, s_{22})^T$, we obtain the state space form

$$\dot{\boldsymbol{m}} = A_m \boldsymbol{m} + v(t)\, \boldsymbol{e}_2, \tag{22}$$

$$\dot{\boldsymbol{s}} = A_s \boldsymbol{s} + Q(m_1, m_2)\, \boldsymbol{e}_3, \tag{23}$$

where $\boldsymbol{e}_2 = (0, 1)^T$, $\boldsymbol{e}_3 = (0, 0, 1)^T$, and

$$A_m = \begin{bmatrix} 0 & 1 \\ -k & -c \end{bmatrix}, \quad A_s = \begin{bmatrix} 0 & 2 & 0 \\ -k & -c & 1 \\ \sigma^2 & p & q \end{bmatrix}, \tag{24}$$

$$Q(m_1, m_2) = \sigma^2 (m_1 - m_2\tau)^2. \tag{25}$$

The most significant feature of this MDE is that the first moment vector $\boldsymbol{m}$ in (22) can be solved by itself and that the second moments $\boldsymbol{s}$ in (23) are affected by the scalar-valued input $Q(m_1, m_2)$ only as shown in Fig.1. This makes this MDE easy to solve.

4.2. **Fundamental harmonic response.** The structure of the MDE shown in Fig.1 allows us to derive the fundamental harmonic response of moments in a rigorous manner as follows. Let us consider the harmonic disturbance

$$v(t) = \cos \omega t, \tag{26}$$

where the amplitude can be assumed to be unity without loss of generality.

4.2.1. *The first moments.* Based on the transfer matrix from $v(t)$ to $\boldsymbol{m}(t)$,

$$\boldsymbol{G}_m(a) = \begin{bmatrix} G_m^1(a) \\ G_m^2(a) \end{bmatrix} = (aI - A_m)^{-1} \boldsymbol{e}_2, \tag{27}$$

we obtain the fundamental harmonic response of the second-order linear system (22) as

$$\begin{aligned}\boldsymbol{R}_m(\omega) &= \begin{bmatrix} R_m^1(\omega) \\ R_m^2(\omega) \end{bmatrix} = |\boldsymbol{G}_m^1(j\omega)| = \frac{1}{\sqrt{(k-\omega^2)^2 + c^2\omega^2}} \begin{bmatrix} 1 \\ \omega \end{bmatrix}, \\ \boldsymbol{\phi}_m(\omega) &= \begin{bmatrix} \phi_m^1(\omega) \\ \phi_m^2(\omega) \end{bmatrix} = \angle \boldsymbol{G}_m^1(j\omega) = \begin{bmatrix} -\arctan\frac{c\omega}{k-\omega^2} \\ \arctan\frac{k-\omega^2}{c\omega} \end{bmatrix}, \end{aligned} \tag{28}$$

where $j = \sqrt{-1}$. Therefore, the fundamental harmonic response of the first moment is obtained as

$$m_i(t) = R_m^i \cos\{\omega t + \phi_m^i\} \qquad (i = 1, 2). \tag{29}$$

4.2.2. *The quadratic element.* Substituting the first moments in (29) into the quadratic function $Q(m_1, m_2)$ in (25), we obtain

$$Q(m_1, m_2) = R_Q(\omega) + R_Q(\omega)\cos\{2\omega t + \phi_Q(\omega)\}, \tag{30}$$

$$R_Q(\omega) = R_m^1(\omega)^2 \, \frac{\sigma^2}{2}\Big(1 + (\omega\tau)^2\Big), \tag{31}$$

$$\phi_Q(\omega) = 2\phi_m^1(\omega) + \arctan\frac{2\omega\tau}{1-(\omega\tau)^2}. \tag{32}$$

Therefore, it appears that the output of the quadratic element is a harmonic function having the doubled frequency 2ω and the drift term $R_Q(\omega)$.

4.2.3. *The second moments.* We now rewrite the equation of second moments in (23) around the static equilibrium $\bar{\boldsymbol{s}}$ satisfying

$$\boldsymbol{0} = A_s\bar{\boldsymbol{s}} + R_Q(\omega)\,\boldsymbol{e}_3. \tag{33}$$

Applying the transformation: $\boldsymbol{s} = \bar{\boldsymbol{s}} + \boldsymbol{s}'$, we obtain the equation of second moments without the drift term:

$$\dot{\boldsymbol{s}}' = A_s\boldsymbol{s}' + w(t)\,\boldsymbol{e}_3, \tag{34}$$

where $w(t) = R_Q(\omega)\cos\{2\omega t + \phi_Q(\omega)\}$ is a harmonic function of the frequency 2ω.

Since the modified equation of the second moment in (34) is a linear system subjected to the harmonic input, we can calculate its harmonic response, using the transfer matrix from $w(t)$ to $\boldsymbol{s}'(t)$ as

$$\boldsymbol{G}_s(a) = (aI - A_s)^{-1}\boldsymbol{e}_3, \tag{35}$$

to obtain

$$\boldsymbol{R}_s'(\omega) = |\boldsymbol{G}_s(2j\omega)|, \quad \boldsymbol{\phi}_s'(\omega) = \angle\boldsymbol{G}_s(2j\omega), \tag{36}$$

where representing their vector components are omitted to save space.

Therefore, the total contribution in amplitude and phase-shift from the disturbance $v(t)$ in (26) to the second moment $\boldsymbol{s}'(t)$ is given by

$$\boldsymbol{R}_s(\omega) = R_Q(\omega)\boldsymbol{R}_s'(\omega), \quad \boldsymbol{\phi}_s(\omega) = \phi_Q(\omega)(1,1,1)^T + \boldsymbol{\phi}_s'(\omega). \tag{37}$$

In summary, we have derived the fundamental harmonic response of moments as in (28) and (37) without approximations, based on the particular structure of our MDE shown in Fig.1.

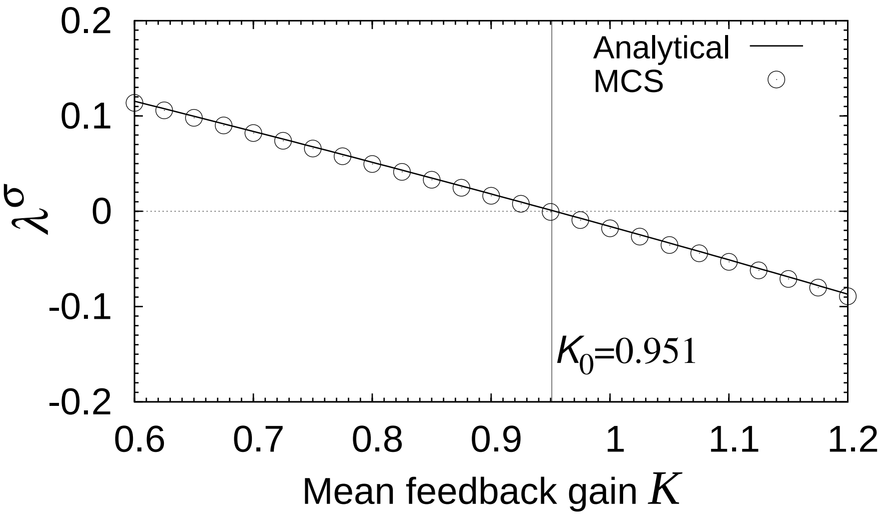

FIGURE 2. Lyapunov exponent λ^σ as a function of the mean feedback gain K for $\zeta = 1.5$ and $\sigma = 0.5$.

4.3. **Robust analysis of moments.** Now we can define the H_∞ norm of moments from the harmonic response obtained above. This enables us to evaluate the robustness of moments against the disturbance $v(t)$. Since all of the transfer functions obtained above are vectors, the H_∞ norm of moments is simply defined by choosing the maximal component of the supremal amplitude vector. In this way, the H_∞ norm of moments is given by

$$H_\infty^\alpha = \max_i \left\{ \left[\sup_\omega \boldsymbol{R}_\alpha(\omega) \right]_i \right\} \quad (\alpha = m, s), \tag{38}$$

where $[\boldsymbol{v}]_i$ denotes the ith component of vector $\boldsymbol{v}$.

On the other hand, all components of the phase-shifts, $\boldsymbol{\phi}_m(\omega)$ and $\boldsymbol{\phi}_s(\omega)$, are monotonically decreasing functions of ω whose infimal values are negative constants independent of the system parameters, i.e., $\inf_\omega \boldsymbol{\phi}_m(\omega) = (-\pi, -\pi/2)^T$, $\inf_\omega \boldsymbol{\phi}_s(\omega) = (-4.5\pi, -4\pi, -3.5\pi)^T$. This means that the dependency on the system parameters cannot be evaluated by a scalar index. To avoid this problem, we evaluate the maximal phase-shift at ω by taking the negative maximum of components as follows:

$$\phi_\infty^\alpha(\omega) = -\max_i \left\{ \left[-\boldsymbol{\phi}_\alpha(\omega) \right]_i \right\} \quad (\alpha = m, s). \tag{39}$$

5. **Numerical Results.**

5.1. **On–off intermittency.** Figure 2 shows Lyapunov exponent λ^σ of the model (13) as a function of the mean feedback gain K for $v(t) = 0$, $\tau = 0.04$, $\zeta = 1.5$, and $\sigma = 0.5$, where the solid line represents the analytical result from the formula (15), and the small circles represent the result from Monte Carlo simulation of the random ODE in (9). Note that the values of $\tau = 0.04$ and $\zeta = 1.5$ represent respectively the neural latency 200 ms and the overdamping characteristics of humans [9].

It appears from Fig.2 that $\lambda^\sigma = \lambda^\sigma(K)$ is a monotonically decreasing function of K having a zero near $K = K_0 \approx 0.951$. This is a reasonable result because the Lyapunov exponent λ^σ is a stochastic counterpart to the real part of the eigenvalues. Thus, a sufficiently large feedback gain K can make the real part of the eigenvalues all negative in the deterministic limit $\sigma \to 0$.

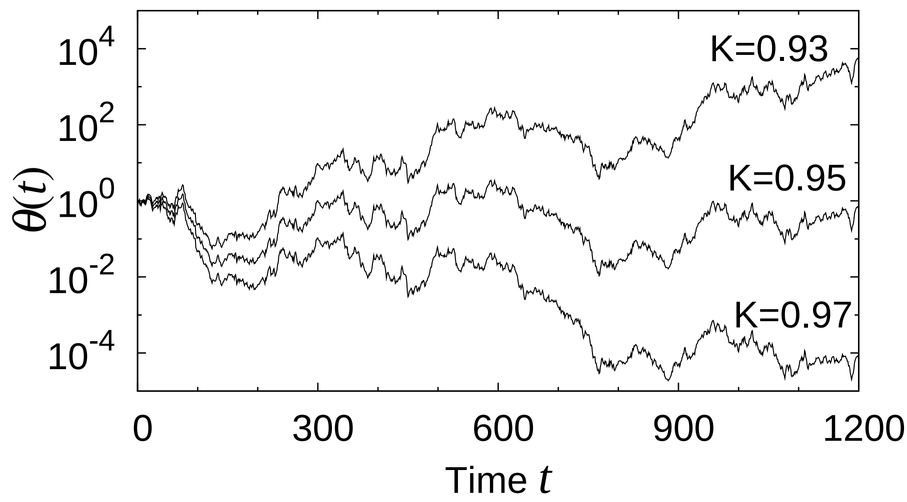

FIGURE 3. Sample paths for $\zeta = 1.5$ and $\sigma = 0.5$.

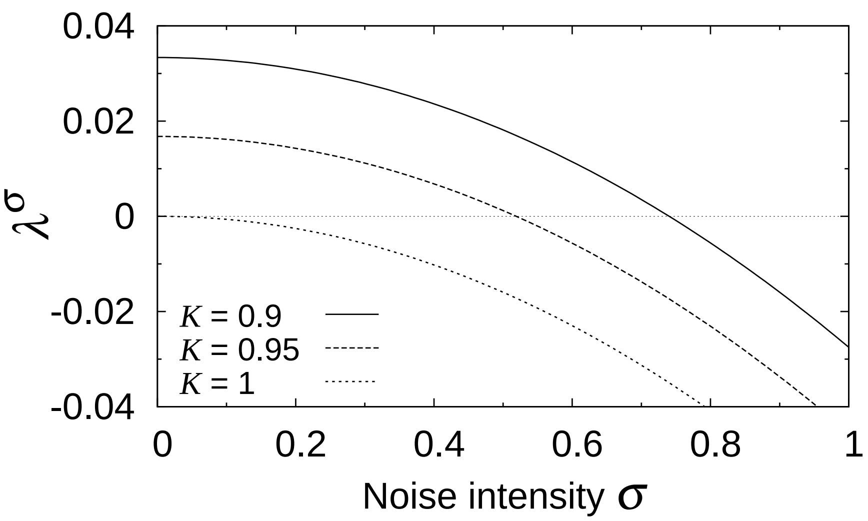

FIGURE 4. Lyapunov exponent λ^σ as a function of the noise intensity σ for $\zeta = 1.5$.

Figure 3 shows sample paths near the zero point $K = K_0$ obtained from the random ODE (9) where the selection of the sample of the noise w_t is identical across cases. It appears that the state $\theta(t)$ is diverging for the smaller gain $K = 0.93 < K_0$ and is converging for the larger gain $K = 0.97 > K_0$. On the other hand, near the zero point $K = 0.95 \approx K_0$, the bounded state wandering in a neighborhood of $|\theta(t)| \approx 10^0$ appears, which is the on–off intermittent behavior we will consider.

For reference, Fig.4 shows the dependency of the Lyapunov exponent λ^σ upon the noise intensity σ. This result can be regarded as an example of noise-induced order [8] because λ^σ, instability, is a monotonically decreasing function of σ and is structurally stable with respect to the change of mean feedback gain $K = 0.9, 0.95, 1$.

5.2. **Amplitude of moments.** Figure 5 shows Lyapunov exponent λ^σ and H_∞ norms as functions of the mean feedback gain K for $\sigma = 0.5$, where $H_\infty(K)$ is calculated following the definition (38). One can easily see that $H_\infty(K)$ is a quasiconcave function of K, whose peak is at $K = K_p$ larger than the zero point $K = K_0$.

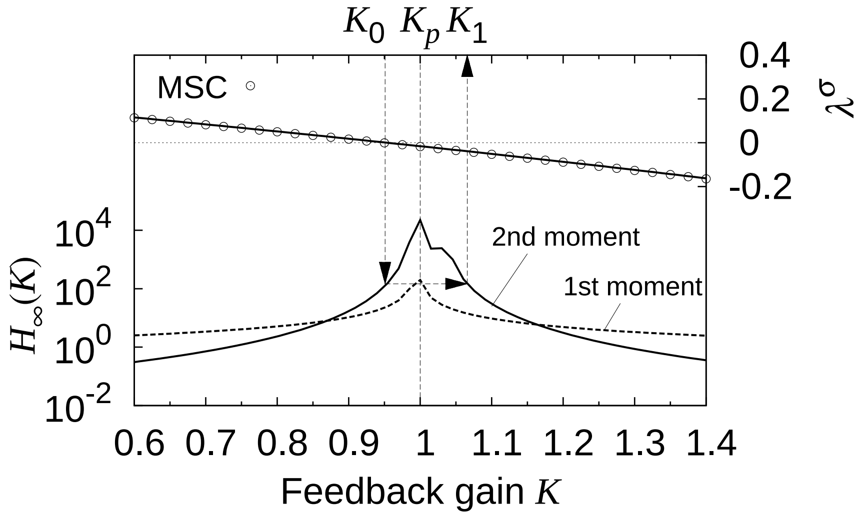

FIGURE 5. Lyapunov exponent λ^σ and H_∞ norms as functions of the mean feedback gain K for $\sigma = 0.5$.

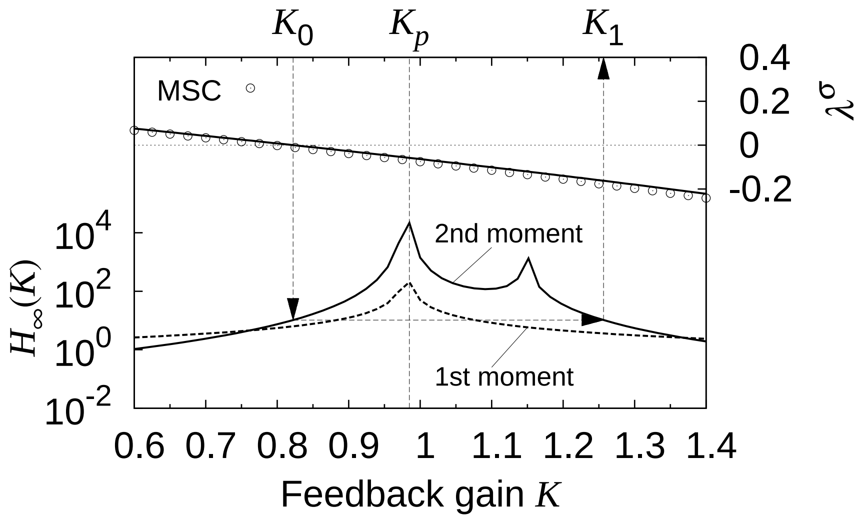

FIGURE 6. Lyapunov exponent λ^σ and H_∞ norms as functions of the mean feedback gain K for $\sigma = 1$.

This result allows us to provide a possible explanation for the human preference for the minimally stable mean feedback gain K_0. It clearly appears in Fig.5 that the gain K_0 locally minimizes $H_\infty(K)$ under the constraint $\lambda^\sigma(K) < 0$ to avoid dynamic instabilities. Therefore, it seems that the gain K_0 preferred by humans locally maximizes the robustness of the moments $\boldsymbol{m}, \boldsymbol{s}$ (actually $\boldsymbol{s}'$). The same consideration applies to the larger noise intensity $\sigma = 1$, as shown in Fig.6.

However, this explanation is limited to a local domain of K because the same robustness can be found globally at

$$K_1 = H_\infty^{-1}\big(H_\infty(K_0)\big) \tag{40}$$

as shown in Fig.5 and 6. Since the second typical gain K_1 provides the same extent of $H_\infty(K)$, or robustness, a human could prefer K_1 without changing the robustness. Furthermore, the second gain K_1 provides stronger asymptotic stability than K_0.

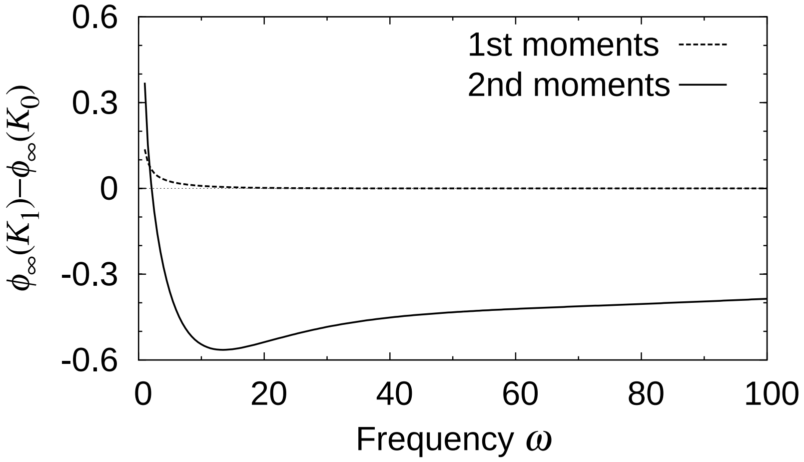

FIGURE 7. Difference between the maximal phase-shifts at $K = K_0$ and K_1 for $\sigma = 0.5$.

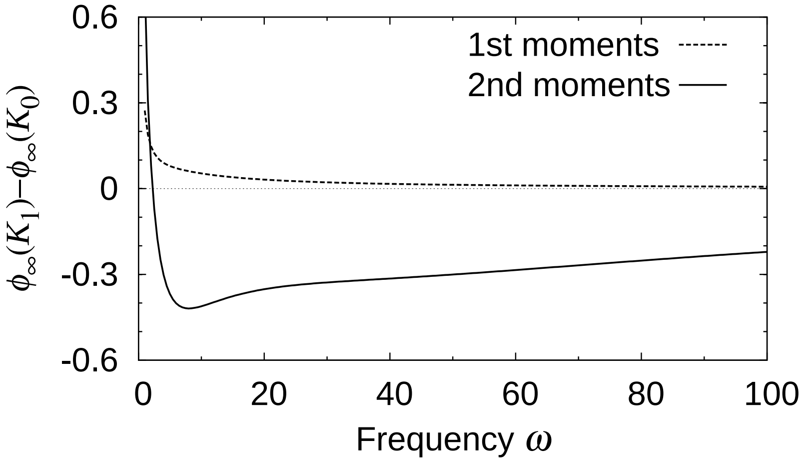

FIGURE 8. Difference between the maximal phase-shifts at $K = K_0$ and K_1 for $\sigma = 1$.

5.3. **Phase-shift of moments.** One explanation to answer the selection of the minimally stable gain K_0 can be obtained by investigating the phase-shift of moments defined in (39) as follows.

Figure 7 shows the difference of maximal phase-shifts between $K = K_0$ and K_1 for $\nu = 0.5$ as a function of the input frequency ω of the disturbance $v(t)$ in (26). It is clearly shown in Fig.7 that switching the gain from K_0 to K_1 results in a significant increase in the maximal phase-shift of second moments.

This result implies that the minimally stable gain K_0 preferred by humans produces a phase-shift significantly smaller than the more stable gain K_1. The same conclusion can be obtained from the different extent of noise $\sigma = 1$, as shown in Fig.8.

6. **Conclusion.** The results obtained in this paper lead to the conclusion that the minimally stable condition K_0 can be characterized as a special condition that minimizes the magnitude of the maximal amplitude H^s_∞ and phase-shift ϕ^s_∞ of second moments subject to the constraint $\lambda^\sigma < 0$ to avoid dynamic instabilities. Since the amplitude of second moments represents the predictability of system responses and the phase-shift of the second moments evaluates the lead time of the dynamic change of the predictability, we may

propose the stochastic explanation that humans prefer better predictability and faster cognition of system response (smaller phase-shift of second moments) while accepting the minimally stable responses.

In future research, we plan to expand our stochastic method into the coupled problem in which multiple human subjects maintain their balance in cooperation with each other.

Acknowledgment. This work was supported by KAKENHI (21560231).

REFERENCES

[1] Juan L. Cabrera and Jhon G. Militon. On-off intermittency in a human balancing task. *Physical Review Letters*, vol. 89, no. 15, pp. 158702:1–4, 2002.
[2] Juan Luis Cabrera and John G. Milton. Human stick balancing: Tuning Lévy flights to improve balance control. *Chaos*, vol. 14, no. 3, pp. 691–698, 2004.
[3] Shankar C. Venkataramani, Thomas M. Antonsen Jr., Edward Ott, and John C. Sommerer. On-off intermittency: Power spectrum and fractal properties of time series. *Physica D*, vol. 96, pp. 66–99, 1996.
[4] J. J. Collins and C. J. De luca. Random walking during quiet standing. *Physical Review Letters*, vol. 73, no. 5, pp. 764–767, 1994.
[5] Michael Lauk, Carson C. Chow, Ann E. Pavlik, and James J. Collins. Human balance out of equilibrium: Nonequilibrium statistical mechanics in posture control. *Physical Review Letters*, vol. 80, no. 2, pp. 413–416, 1998.
[6] Attila Priplata, James Niemi, Martin Salen, Jason Harry, Lewis A. Lipsitz, and J. J. Collins. Noise-enhanced human balance control. *Physical Review Letters*, vol. 89, no. 23, pp. 238101:1–4, 2002.
[7] Toru Ohira and Yuzuru Sato. Resonance with noise and delay. *Physical Review Letters*, vol. 82, no. 14, pp. 2811–2815, 1999.
[8] K. Matsumoto and I. Tsuda. Noise-induced order. *Journal of Statistical Physics*, vol. 31, no. 1, pp. 87–106, 1983.
[9] John Milton, Juan Luis Cabrera, Toru Ohira, Shigeru Tajima, Yukinori Tonosaki, Christian W. Eurich, and Sue Ann Campbell. The time-delayed inverted pendulum: Implications for human balance control. *Chaos*, vol. 19, pp. 206110:1–12, 2009.
[10] Katsutoshi Yoshida and Yusuke Nishizawa. Convergence property of noise-induced synchronization. *International Journal of Innovative Computing, Information and Control*, vol. 4, no. 1, pp. 79–89, 2008.
[11] Katsutoshi Yoshida and Yusuke Nishizawa. Bifurcation analysis of noise-induced synchronization. *International Journal of Innovative Computing, Information and Control*, vol. 5, no. 9, pp. 2809–2818, 2009.
[12] Katsutoshi Yoshida, Atsushi Higeta, and Shinichi Watanabe. Effects of mechanical coupling on the dynamics of balancing tasks. *International Journal of Innovative Computing, Information and Control*, vol. 7, no. 3, 2011. in printing.
[13] Md. Zahidul Islam, Chi-Min Oh, and Chil-Woo Lee. An efficient multiple cues synthesis for human tracking using a particle filtering framework. *International Journal of Innovative Computing, Information and Control*, vol. 7, no. 6, pp. 3379–3393, 2011.
[14] Catalin Buiu and Nirvana Popescu. Aesthetic emotions in human-robot interaction. implications on interaction design of robotic artists. *International Journal of Innovative Computing, Information and Control*, vol. 7, no. 3, pp. 1097–1107, 2011.
[15] Yoichiro Maeda and Ryohei Taki. Interactive emotion communication between human and robot. *International Journal of Innovative Computing, Information and Control*, vol. 7, no. 5(B), pp. 2961–2970, 2011.
[16] L. Arnold, M. M. Doyle, and N. Sri Namachchivaya. Small noise expansion of moment Lyapunov exponents for two-dimensional system. *Dynamical Systems*, vol. 13, no. 3, pp. 187–211, 1997.
[17] G. W. Gardiner. *Handbook of Stochastic Methods for Physics, Chemistry, and the Natural Science.* Springer, second edition, 1985.
[18] M. S. Fofana. Asymptotic stability of a stochastic delay equation. *Probabilistic Engineering Mechanics*, vol. 17, pp. 385–392, 2002.